Single-Molecule Imaging of the Association of the Cell-Penetrating Peptide Pep-1 to Model Membranes†

Alexey Sharonov and Robin M. Hochstrasser*

Department of Chemistry, University of Pennsylvania, Philadelphia, Pennsylvania 19104-6323

Received March 13, 2007; Revised Manuscript Received April 27, 2007

ABSTRACT: Pep-1 is an amphiphatic peptide that can form noncovalent complexes with a cargo protein with subsequent delivery into a live cell. In this study, the behavior of Pep-1 was directly visualized by fluorescent imaging techniques at the single-molecule level of sensitivity. The interactions of Pep-1 and two of its labeled fluorescent analogues with large and cell-sized giant unilamellar vesicles and supported bilayers are reported. The role of the bilayer charge and ionic strength of the medium were examined. Pep-1 caused fusion and association of vesicles, and it perturbed the vesicle's membrane. The association of the peptide with neutral bilayers was promoted by anchoring of the cysteamine moiety. The association of the peptide with the structural defects of the neutral membrane was very efficient. The electrostatic forces were shown to be important for the association of the peptide only in low ionic strength solutions and were completely diminished at physiological ionic strength. Pep-1 did not induce the association to the model membrane of a number of proteins chosen to exhibit a range of properties. The results suggest that Pep-1 assisted delivery of cargo in living cells may result from cooperative effects.

The efficient delivery of macromolecules into living cells is important for therapeutic purposes. Many transfection techniques have been developed including microinjection, electroporation, and delivery by intermediate agents such as cationic liposomes and viral vectors. The discovery of a class of peptides, known as cell-penetrating peptides (CPP),[1] with the ability to mediate translocation of various cargoes both in vitro and in vivo has provided a new approach to delivery (*1*). Recently, an amphiphatic peptide having 21 residues, Pep-1, was developed that is able to deliver cargo proteins into several cell lines without the need for covalent coupling (*2*). Pep-1, known commercially Chariot (*3*), is a synthetic peptide carrier that contains a hydrophobic, tryptophan-rich domain and a hydrophilic portion that is rich in basic amino acids. These domains are separated by a short spacer. The hydrophilic sequence improves the solubility, and the spacer domain provides a flexible link between the two domains. The ability of Pep-1 to translocate a cargo protein through the plasma membrane has been widely demonstrated (*2*, *4*, *5*). It has been conjectured that a peptide/protein complex is formed by the hydrophobic interactions and that the cargo protein is internalized via the formation of a transient pore in the plasma membrane (*2*).

Pep-1 forms complexes due to its hydrophobic interaction with several proteins such as GFP (*2*) and β-galactosidase (*2*, *4*). Pep-1 also appears to mediate the transport of dextrans under conditions where endocytosis is inhibited (*4*). The ability of Pep-1 to translocate dextran, which is hydrophilic, has suggested that hydrophobicity is not essential for complex formation and cell uptake. Whether formation of complexes is a necessary step in translocation and how the Pep-1 interacts with cargo proteins appear to be unresolved. An important possibility is that the significant excess of Pep-1 often required for protein delivery (*3*, *4*) may induce fusion and aggregation of the lipid membrane (*6*). The formation of Pep-1 induced pores has not been detected in either cell (*4*) or model membranes (*6*, *7*), so the specific nature of any alterations of the plasma membrane integrity that occur when Pep-1 delivers cargo protein requires new experiments. In most of the previous experiments with Pep-1 the internalized proteins do not distribute evenly in the cytosol but appear as punctuated patterns (*2*, *4*, *7*) that may indicate an endocytic rather than nonendocytic pathway of translocation. Two mechanisms are being currently discussed: the energy-independent one (*2*, *4*, *6*, *8*) and the mechanism where Pep-1 forms an invagination in the cell membrane that triggers endocytic uptake (*7*).

Experiments in vivo are often difficult to interpret because of cell treatment, cell autofluorescence, and the heterogeneous nature of the cell. For example, the translocation of proteins in a living cell in the presence of Pep-1 may also involve natural endocytic pathways. It has been shown that experiments with fixed cells or with reduced temperatures may result in conditions (*9*) where endocytic and nonendocytic pathways cannot be easily distinguished. Therefore, it seemed that there is a need for an evaluation of the properties of Pep-1 in model systems such as vesicles and lipid bilayers that are relatively well-defined structurally yet share characteristics with cell membranes. Experiments

†This research was supported by Grant RFA-RM-04-001 with instrumentation from NIH RR 01348.

* To whom correspondence should be addressed. E-mail: hochstra@sas.upenn.edu. Phone: 215-898-8410. Fax: 215-898-0590.

[1] Abbreviations: CPP, cell-penetrating peptide; POPC, 1-palmitoyl-2-oleoyl-*sn*-glycero-3-phosphocholine; POPS, 1-palmitoyl-2-oleoyl-*sn*-glycero-3-phosphoserine; NBD, nitrobenzoxazole; TCEP, phosphine hydrochloride; LUV, large unilamellar vesicle; GUV, giant unilamellar vesicle; DIC, differential interference contrast; TIRFM, total internal reflection fluorescence microscopy.

10.1021/bi700505h CCC: $37.00
Published on Web 06/13/2007

Table 1: Amino Acid Sequences and Molecular Weights of the Peptides

name[a]	sequence[a]	molecular mass, Da (MALDI-MS)
Pep-1	Ac-KETWWETWWTEWSQPKKKRKV-Cya	2949.8
AF-Pep	Ac-KETWWETWWTEWSQPKKKRKV-AF	3649.6
HL-Pep	HL-LC-KETWWETWWTEWSQPKKKRKV-Cya	3377.3

[a] Abbreviations: Ac, N-terminal acetylation; Cya, cysteamine; HL, Hilyte Fluor 488 dye; AF, Alexa Fluor 488 dye; LC, 6-aminohexanoic acid.

performed on model membranes have shown that Pep-1 has a high affinity for lipid bilayers [$K_p \sim 10^3-10^4$ (*6*)] in which the hydrophobic domain of Pep-1 adopts an α-helical conformation (*2*, *7*). It has been suggested that the membrane crossing process might not involve formation of a transient transmembrane pore-like structure (*8*). Pep-1 induced translocation was observed for negative transmembrane potentials and involved transient fusion to the membrane (*6*). The hypothesis that the transmembrane potential is a driving force for translocation has not been widely adopted, and it has even been proposed that Pep-1 does not actually cross the membrane but causes a distortion of the bilayer resulting from the hydrophobic and electrostatic interactions (*7*).

Previous measurements involving Pep-1 in vitro have been carried out in LUV suspensions or in lipid bilayers at air/water interfaces using bulk fluorescence methods. In the present paper, we have concentrated on direct methods of detection at the single-molecule level. Novel imaging methods were used to examine alterations in membrane structure, association of fluorescently labeled peptide and several proteins with supported bilayers, LUVs and GUVs, and peptide-induced association of proteins to these lipids.

MATERIALS AND METHODS

Materials. Lipids (POPC, 16:0−18:1 PC 1-palmitoyl-2-oleoyl-*sn*-glycero-3-phosphocholine; POPS, 16:0−18:1 PS 1-palmitoyl-2-oleoyl-*sn*-glycero-3-[phospho-L-serine]; and NBD, 6:0-N-NBD 1-oleoyl-2-[6-[(7-nitro-2,1,3-benzoxadiazol-4-yl)amino]hexanoyl]-*sn*-glycero-3-phosphocholine) were purchased from Avanti Polar Lipids; Hepes buffer, sodium chloride, and sucrose were from Fisher Chemical, and chloroform was from Acros Organics. D-(+)-Glucose was from Sigma. 5,5′-Dithiobis(2-nitrobenzoic acid) (Ellman's reagent) was purchased from Pierce Chemical Co.

The Alexa Fluor 568 conjugate of transferrin from human serum, ovalbumin, Texas Red conjugate, the Alexa Fluor 568 $F(ab')_2$ fragment of goat anti-mouse IgG, and the reducing agent tris(2-carboxyethyl)phosphine hydrochloride (TCEP) were from Invitrogen.

Glass coverslips and cylinders (Fisher) were cleaned by sonication for 1 h in Piranha solution (3:1 mixture of sulfuric acid and 30% hydrogen peroxide) with sequential extensive washing in UltraPure water (Millipore Corp.).

Peptide Synthesis and Labeling. The amino acid sequences and molecular weights of Pep-1 and two fluorescently labeled analogues of Pep-1 are listed in Table 1.

Pep-1. The Chariot transfection reagent was purchased from Activemotif (Carlsbad, CA). Although the manufacturer does not give the sequence and molecular weight, the equivalence of Pep-1 and Chariot is widely accepted (*4*, *6*, *7*, *10*). We confirmed the presence of the cysteamine group at the C-terminus of Chariot by the reaction with Ellman's reagent. The mass spectrum of Chariot was also in agreement with expectations calculated from the amino acid sequence.

AF-Pep. The conjugation reaction of Chariot (Pep-1) with thiol-reactive dye [Alexa Fluor 488 C_5 maleimide (Invitrogen)] was carried out in accordance with the manufacturer's protocol. The conjugate was separated by gel filtration (NAP-5; GE Healthcare) with careful monitoring of the elution profile in the whole UV−vis spectral range. The degree of labeling was determined to be close to one dye/peptide. Both spectroscopic analysis and MALDI-MS confirmed the high purity of labeled peptide (labeled/unlabeled >9:1) and the absence of nonconjugated dye in the final solution.

It has been reported that properties of Pep-1 are modified by labeling the C-terminus (*7*, *10*, *11*). This prompted us to design an alternative labeling of the peptide. We introduced a label at the N-terminus via a long-chain linker to minimize the effect of fluorescent dye on the peptide properties. Hilyte Fluor 488 labeled peptide was synthesized and HPLC purified to >95% by AnaSpec, Inc. (San Jose, CA).

Large Unilamellar Vesicle (LUV) Preparation. Large unilamellar vesicles were prepared by the standard extrusion technique (*12*). Briefly, 0.1 mL of 10 mg/mL lipids in chloroform was evaporated by nitrogen flow in a small glass vial to yield a dry phospholipid film. After drying for 1 h in vacuum, the film was hydrated in 1 mL of 10 mM Hepes buffer, pH 7.4, with continuous stirring at room temperature for 1.5 h. After five freeze/thaw cycles the resulting multilamellar vesicles were extruded 21 times through 100 nm polycarbonate membranes (Whatman) by means of a miniextruder (Avanti Polar Lipids).

Giant Unilamellar Vesicle (GUV) Preparation. The GUVs were prepared in a standard manner. Briefly, 10 μL of 0.2 mg/mL lipid solution in chloroform was deposited on indium tin oxide (ITO) coated glass and subsequently dried by a nitrogen flow and in vacuum for 1 h. The GUVs were grown in an electric field as described in ref *13*. Two ITO coated glass plates separated by a 2 mm rubber spacer formed the preparation chamber. A 10 Hz sinusoidal voltage was applied to the electrodes at 0.5 V/mm while the chamber was filled with either 0.2 M sucrose solution or pure water. The electric field was gradually raised up to 1.5 V/mm in steps of 0.1 V, applied every 5 min by means of a function generator, based on an NI-DAC board (National Instruments). The growth of the vesicles was visually monitored by differential interference contrast (DIC) microscopy. Vesicle formation was continued for 1 h at 1.5 V/mm. The GUVs were then gently removed by a syringe and stored at 4 °C.

Sample Preparation. The properties of the bilayer were varied by mixing neutral and anionic lipids (POPC and POPS) in different proportions. In some experiments the lipid mixture contained 0.25% NBD-labeled material in order to visualize the bilayer by fluorescence microscopy.

One microliter of LUV or GUV suspension was added to a 100 μL chamber (cell separation glass cylinder located on a microscope glass slide). The chamber was filled with a solution having a similar interior osmolarity to the GUV and then adjusted by addition of an appropriate amount of glucose in NaCl (or KCl), 10 mM Hepes (pH = 7.4) buffer. The ionic strength of the solution was variable from zero to physiological (150 mM). Due to differences in the densities of the solutions in the interior and exterior of the GUV, it sank to the bottom of the glass vessel and either attached to the surface or spontaneously ruptured. The extensive agitation of the GUV sample led to the formation of the uniformly supported bilayers used in our experiments.

Microscope. The setup, based on a commercial Olympus IX81 inverted microscope, was in part described previously (*14*−*16*). The laser beams from Ar^+ (488 nm) and Kr^+ (568 nm) ion lasers pass through two independent excitation channels. Each channel consists of a quarter-wave plate to generate circularly polarized light, expansion optics, mechanical PC controlled shutter, and appropriate lenses to focus excitation onto the back focal plane of an oil immersion objective (Olympus 60× NA = 1.45). A lens, coupled with a translation stage, was used to align the excitation beam across the objective's back aperture to achieve easy illumination, angle adjustment, and interconversion of the setup between through-the-objective TIR and epifluorescence microscopy. The excitation light was filtered by appropriate laser band-pass filters and dichroic mirrors (Chroma). Fluorescence from the sample was collected by the objective and directed to a CCD camera with multiplication-on-chip capability (Roper Scientific, Cascade 512F) by means of a beam splitter and an appropriate set of band-pass filters (Omega Optical). With the 1.6× lens the total magnification of the microscope was 96×, which yields a pixel size in the image plane of the camera of ∼167 nm. Time-lapsed image recording and control of the microscope were performed by especially designed LabView (National Instruments) based software. The recorded sequences of frames were analyzed by in-house developed software based on MATLAB (The MathWorks Inc.). All experiments were conducted at room temperature. The binding of the fluorescently labeled peptides was detected by measurement of the fluorescence associated with the peptide label.

The sensitivity of our microscope was high enough to detect single fluorophores that were immobilized for more that 10−20 ms as shown previously with this same setup (*16*). The framing rate in the experiments was 20−50 ms/frame. Single-step photobleaching was checked in all of the experiments if not otherwise specified. The fluorescence shown in the figures and discussed in the Results section was obtained by averaging multiple frames. Usually 50−100 frames or more were averaged.

TIRFM. In total internal reflection (TIR) geometry excitation evanescent field localized within a few hundred nanometers from the surface of interface, and observation of single fluorescent molecules is possible even in a high fluorescent environment (*17, 18*). We applied this technique for studying the adsorption to supported lipid bilayers.

Low-Angle Epiillumination. The evanescent wave in TIRFM does not penetrate far enough from the glass/media interface to permit observations of regions other than the surface. We developed a new excitation scheme for imaging optical cross sections in a low-angle epiillumination (or grazing angle) configuration of excitation which allows visualization and recording of single molecules far away from the interface. Objects are illuminated with a laser beam directed at a very low angle to the interface; this approach permits excitation of relatively thin layers (typically 7−10 μm thickness). The focus depth of our objective is about 1−1.5 μm so only molecules localized in the 1−1.5 μm cross section appear as diffraction-limited spots. The imaged slices can be separated from the surface by as much as 150 μm. The advantage of this method is low background which allows visualization of single molecules at some distance from the interface even in fluorescent solutions.

RESULTS

Pep-1 Induced Fusion and Sedimentation of LUVs. POPC/POPS/NBD LUVs (4:1) were immersed in 150 mM KCl buffer at a final concentration of 5×10^{-10} M. The effect of addition of Pep-1 on the free-floating vesicles was monitored in the grazing angle geometry. Immediately after addition of the peptide (final concentration 0.8 μM) vesicles tended to aggregate into larger ones characterized by higher intensities of fluorescence and smaller coefficients of diffusion.

Sedimentation of vesicles onto a clean glass interface in the presence and absence of 1.1 μM Pep-1 was monitored in the TIRFM mode. After incubation for 20 min, the vesicles uniformly cover the glass surface; however, some properties of lipids in the layers were very different in the presence of the peptide.

The fluorescent images of the glass/medium interface taken at 50 ms exposure are shown in Figure 1. The left column (Figure 1a,c) shows photobleached samples (0 s). The right column of images (Figure 1b,d) are the same areas but after 60 s in the dark. When no Pep-1 was present, no fluorescence recovery after photobleaching (FRAP) was detected; vesicles contact the surface transiently and appear as fluorescent spots in the image (Figure 1d). This indicates that neighboring vesicles at the glass surface are not connected. On the contrary, when the peptide was added to the vesicle suspension, the lipids form a uniform bilayer on the glass surface. After photobleaching the fluorescence recovers because of diffusion of labeled lipids from nonexposed areas of the bilayer (Figure 1b). The kinetics of the FRAP is shown in Figure 1e. The diffusion coefficient, determined as described in ref *19*, was ca. 3 $\mu m^2/s$, which is typical for a supported bilayer in the liquid phase (*20*). Therefore, in the presence of Pep-1 the vesicles attach permanently to the surface and fuse into a preformed bilayer.

Experiments on adsorption of fluorescently labeled peptides HL-Pep and AF-Pep to the glass surface were also carried out. These peptides readily adsorb to glass. After several minutes a large enough fraction of the peptide was bound to the glass surface that the concentration of the free peptide in the sample chamber was significantly reduced. This adsorption is understood to be a result of Pep-1 being a positively charged peptide at pH = 7.4 that binds to the negatively charged groups of the glass. The sedimentation of the vesicles and Pep-1 adsorption to the glass surface reduce both their concentrations to an extent that could readily affect the results of bulk measurements on dilute solutions in glass containers.

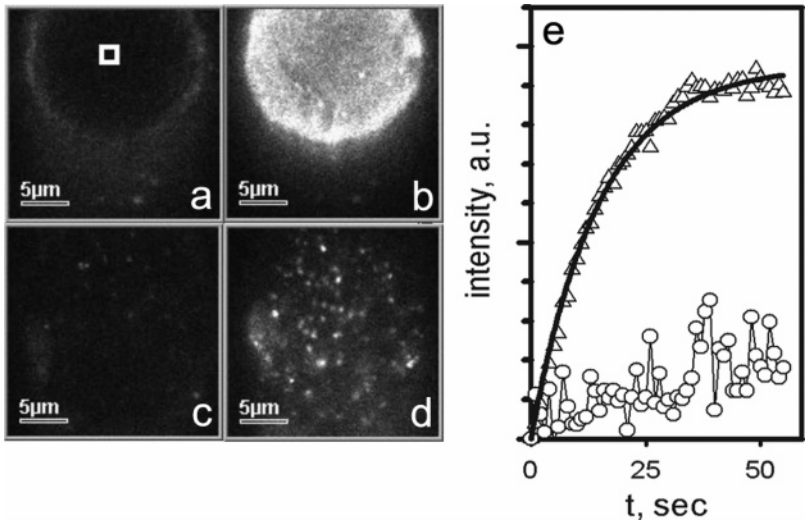

FIGURE 1: Formation of the uniform bilayer induced by Pep-1. POPC/POPS (4:1) LUVs labeled with NBD (0.25% molar ratio) were immersed in buffer in the presence (a, b) and absence (c, d) of 1.2 μM Pep-1. After photobleaching (a, c) fluorescence recovers (b) when Pep-1 is present due to diffusion of labeled lipids from nonexposed areas. Without Pep-1 LUVs transiently touch the surface (d), but no fusion of LUVs was detected. (e) The kinetics of recovery from data in the central area identified by the square in (a). The solid line is fit to experimental kinetics (triangles) with Pep-1, and the circles are data without Pep-1.

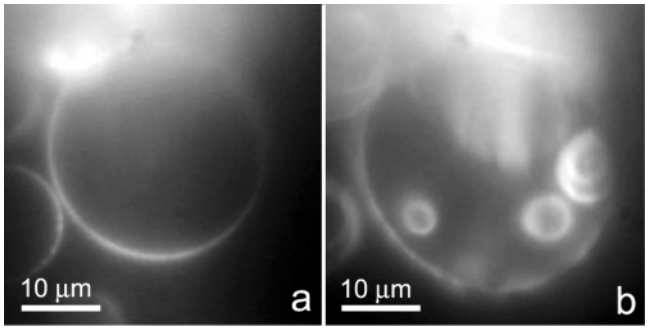

FIGURE 2: Perturbations caused by Pep-1 on GUV membranes. Giant vesicles of POPC/POPS/NBD (4:1, 0.25% of NBD) in pure water before (a) and after (b) addition of Pep-1 at 1.2 μM. Changes in the membrane of the GUVs lead to the formation of multiple internal vesicles, often multilamellar ones.

Pep-1 causes changes in membranes and disruption of GUVs. The GUVs were used to examine the effect of the peptide on lipid membrane organization. Figure 2 shows the equatorial cross section of fluorescently labeled GUVs. Addition of 1.2 μM Pep-1 to the GUV formed from POPC/POPS/NBD with pure water inside and outside leads to the formation of smaller, often multilamellar vesicles inside the GUV. A similar effect was observed for a sucrose-loaded POPC/POPS/NBD 2:1 GUV immersed in glucose solution. Addition of 0.2 μM HL-Pep caused fusion of two GUVs and the formation of a smaller vesicle inside. Often smaller vesicles formed on the surface of the membrane. These small vesicles migrated slowly on the surface of the GUV. Higher concentrations of Pep-1 (>10 μM) completely disrupt almost all of the GUVs. The vesicles filled with sucrose solution were more stable than those containing pure water, probably because of the more viscous environment.

Pep-1 Adsorption to GUV Membranes. GUVs represent an exellent model of a free-standing membrane because their interaction with the support involves only the lower part of the vesicle, while most of the surface of a spherical GUV is free from any type of interaction with the glass. The association of the peptides and proteins to the artificial GUV membrane was monitored in the grazing angle epiillumination geometry by means of optical cross sectioning of the GUVs. The diameters of the GUVs were in range of 20−30 μm, and equatorial cross sections were located at a distance of 10−15 μm from the glass support, eliminating the effects of undesirable artifacts due to interaction with charged groups at the glass surface.

The binding of Pep-1 fluorescently labeled at the C-terminus (AF-Pep) to the GUV membrane was studied in the grazing angle geometry in various environments and anionic lipid concentrations. We imaged equatorial cross sections of sucrose-loaded GUVs immersed in either neutral (no salt) or ionic (7−150 mM NaCl) peptide solutions. The labeled AF-Pep (final concentration 0.1 μM) was added to the sample chamber containing the appropriate buffer and equilibrated for 10 min at which point GUVs consisting of either neutral (POPC) or anionic (POPC/POPS) lipids were added into the chamber. The sedimentation of the GUV to the glass interface and association of the peptide with the bilayer took place over a period of about 15 min. Randomly chosen GUVs were first located by differential image contrast (DIC) microscopy to prevent photobleaching of the fluorophore during the optical adjustments. Finally, the membrane-bound peptide fluorescence was measured and the background signal subtracted. Measurements were repeated for five to seven GUVs having similar size and then averaged. The absence of AF-Pep fluorescence on the membrane surface showed that there was no association of the AF-Pep with the neutral membrane in either low or high ionic strength solution (Figure 3a). The peptide does bind to the anionic bilayer (Figure 3b) in the ion-free solution; however, this binding was absent at physiological ionic strength. These results demonstrate that AF-Pep-1 binds to the membrane solely as a result of electrostatic attraction to the bilayer and that there is no observable association promoted solely by hydrophobic interactions.

The membrane affinity of Pep-1 labeled at the C-terminus is reduced compared with nonlabeled Pep-1 (*11*). The HL-Pep peptide has a C-terminal cysteamine group similar to the native Pep-1. In contrast to AF-Pep, HL-Pep associates

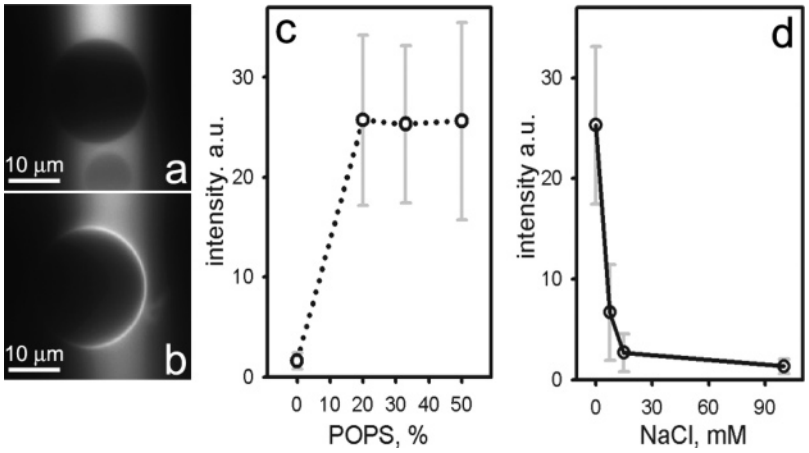

FIGURE 3: Association of fluorescently labeled peptides with the surface of a GUV. (a) Equatorial cross section of the DOPC GUV in 0.2 M glucose. The background fluorescence originates from the free-floating peptides; no binding to the GUV surface is observed. (b) DOPC/DOPS (3:1) in 0.2 M glucose. AF-Pep binds to the charged surface of the GUV. (c) Intensity of fluorescence of bound HL-Pep on the surface of GUV as a function of the anion content of the lipid. (d) Dependence of the association of HL-Pep to the surface of anionic DOPC/DOPS (3:1) GUV on ionic strength. Gray bars represent a standard deviation.

with both the charged and to a minor extent the neutral membrane. The dependence on anionic lipid concentration of the HL-Pep affinity to the membrane in a low ionic strength buffer is shown in Figure 3c. Simplified Gouy−Chapman theory (*21*) predicts that the number of bound peptides should increase exponentially with the mole fraction of the negatively charged lipid in the membrane. The saturation of the charge effect, as shown in Figure 3, originates from the low concentration of the peptide in the solution; the peptide adsorbs not only to the charged membrane but also to the negative groups at the glass surface, reducing the free peptide in the solution. The weak association with the neutral membrane may be caused by the interaction of the tryptophan-rich hydrophobic domain of the peptide facilitated by anchoring of the cysteamine group as proposed in ref *7*. The ionic strength of the solution has a significant effect on the binding efficiency. The dependence of measured surface fluorescence versus concentration of NaCl is shown in Figure 3d. At 100 mM NaCl the concentration of the peptide bound to the GUV surface is significantly reduced and comparable to its binding to the neutral membrane. Thus the ions efficiently shield the electrostatic interaction with the bilayer.

In ref *10* the formation of −S−S− bonds was discussed as having a role in peptide partitioning to the membrane; however, we did not observe any influence of the TCEP reducing agent on binding in either neutral or physiological ionic strength solutions.

In some cases, we observed large clusters of the peptide migrating along the POPC GUV surface (Figure 4). Figure 4 represents the top cross section of the GUV. Bright white spots originate from fluorescence of the labeled peptide. The motion of these spots was recorded at 100 ms/frame during 8 s at 20 ms exposure time. The high fluorescence intensity of the spots arises from clustering of the peptide. The diffusion coefficients obtained by tracking the Brownian motion were determined to be ca. 1.1 $\mu m^2/s$ and 0.9 $\mu m^2/s$ for low-intensity (i.e., small) clusters and 0.3 $\mu m^2/s$ for brighter (larger) ones.

These clusters may occur because of binding of the hydrophobic domain of the peptide to defects in the lipid packaging on the membrane surface. This clustering is a quite rare event, and it does not occur in every studied GUV. We associate this clustering with the defects on the membrane.

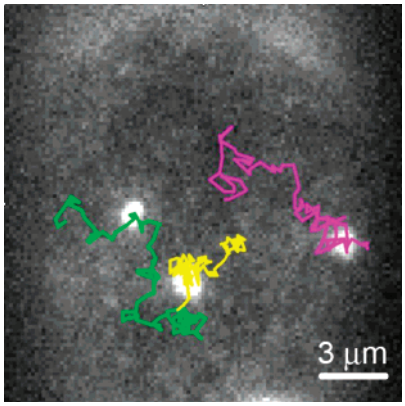

FIGURE 4: Formation of large clusters of HL-Pep on the surface of POPC GUV. Three clusters (white spots) are formed upon addition of the peptide to the solution. The trajectories associated with the diffusion of the clusters are shown by red, green, and yellow lines.

Most importantly, no translocation of the peptide through either the neutral or the symmetrically charged (no transmembrane potential) GUV membrane was observed in these experiments.

Pep-1 Adsorption to Supported Membranes. The supported bilayer remains stable on the glass surface for sufficient time to enable repetitive measurements to be made on the same bilayer at different ionic strengths. The measurements were carried out on one region of the sample by gentle exchange of the surrounding medium without disturbing the supported membrane. Figures 5 and 6 are fluorescence images of the supported bilayers which consist of a number of bilayer islands having a wide range of sizes. These bilayers are either totally exposed (central bilayer in images) or have nonexposed areas (i.e., areas located out of the circular excitation beam). Adsorption of 8×10^{-8} M HL-Pep onto the neutral bilayer (POPC) in both 150 mM NaCl and salt-free buffers showed efficient binding only to the membrane edges: association with the unperturbed membrane was low. This conclusion is clear from the fact that only the membrane contour is well pronounced in the fluorescent image of

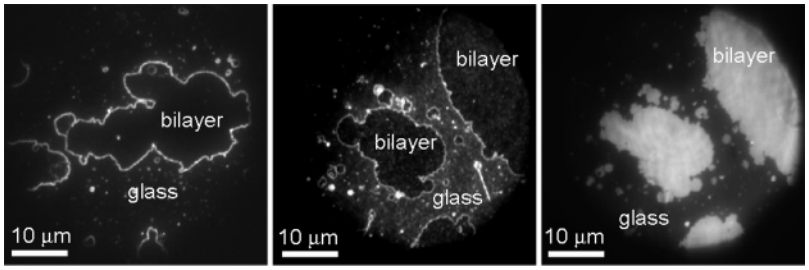

FIGURE 5: Binding of HL-Pep to neutral POPC (a) and anionic POPC/POPS (3:1) (b, c) supported bilayers. 8×10^{-8} M HL-Pep was added into either physiological (0.15 mM NaCl) (a, b) or zero salt (c) 10 mM Hepes buffer.

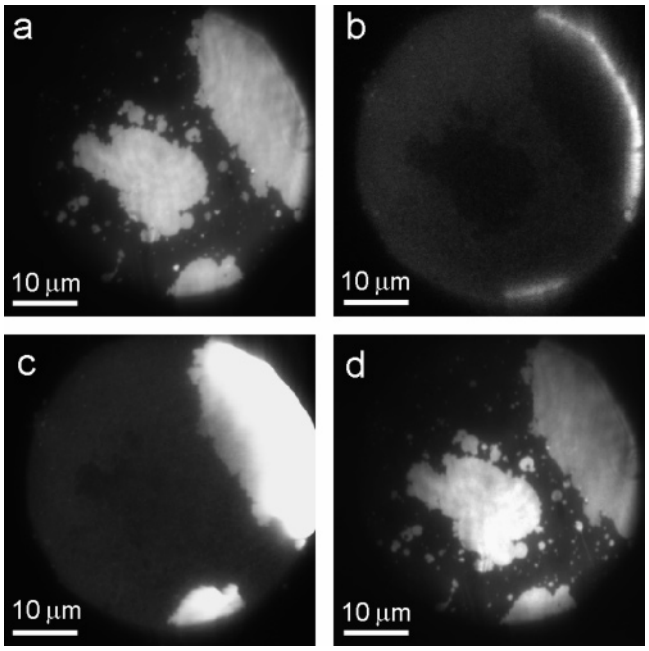

FIGURE 6: Photobleaching and recovery of the fluorescence of HL-Pep in POPC/POPS (3:1) supported bilayers: before photobleaching (a); the same area after photobleaching (b); recovery after photobleaching (140 s) (c); after HL-Pep was again added to the sample chamber (d).

Figure 5a. The efficiency of binding of the HL-Pep to the negatively charged supported bilayer (POPC/POPS, 2:1) is strongly dependent on the ionic strength of the surrounding solution. There is almost no nonedge specific fluorescence at high ionic strength (Figure 5b), while peptides efficiently associate to the entire membrane when no salt is present (Figure 5c). These data support the importance of the electrostatic forces in the association of the peptide with charged membranes. The peptides that electrostatically attach to the bilayer remain permanently fixed to the membrane surface. After photobleaching of HL-Pep in the exposed areas the fluorescence recovers solely by diffusion from nonexposed areas of the bilayer (Figure 6c).

However, the fluorescence of the isolated bilayer close to the center of Figure 6a is not recovered because there is no peptide left in the solution. After addition of a new aliquot of the peptide the fluorescence appears again on all fragments of the membrane (Figure 6d).

Peptide/Protein Interaction. It has been proposed (*2*) that Pep-1 forms a complex with the cargo protein and assists in its translocation through the plasma membrane of the cell. We performed experiments with several mid-sized fluorescently labeled proteins having a range of surface charges and exposed hydrophobic regions. Human transferrin (80 kDa), ovalbumin (40 kDa) and $F(ab)_2$ (50 kDa) were used for our studies of the occurrence of peptide/protein complexes on the surface of the lipid bilayer.

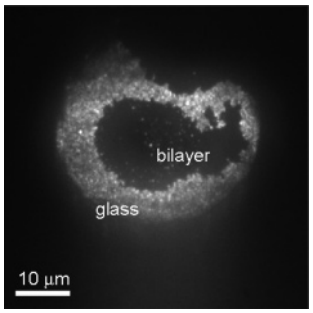

FIGURE 7: POPC supported bilayer in 0.15 M NaCl, Hepes buffer in the presence of Pep-1/transferrin (20:1). The bright signal corresponds to the fluorescence of labeled transferrin adsorbed to the glass surface. No binding to the edge or the surface of the bilayer is seen.

Transferrin does not bind to neutral GUVs or to supported bilayers at any ionic strength, but it weakly binds to negatively charged ones (POPC/POPS, 2:1) in pure water. No association with anionic membranes at physiological ionic strength was detected. Although transferrin is almost electrostatically neutral at neutral pH [isoelectric point of the transferrin is pI = 5.9 (*22*)], its positively charged groups could assist in nonspecific binding to charged membranes. The ability of Pep-1 to assist in binding of transferrin to a lipid bilayer was examined over a range of peptide/protein molar ratios in the range from 20:1 to 80:1. The peptide was incubated with the appropriate amount of protein for 30 min and then added to the sample chamber containing either GUVs or supported bilayers. Similar experiments were performed with Pep-1 and transferrin added sequentially to the sample chamber. The final concentration of transferrin was kept at 1.2 μM. We did not detect any Pep-1 induced association of the transferrin with either the neutral or ionic membrane in experiments conducted at physiological ionic strength. Also in pure water, no association of the transferrin to the POPC bilayer was observed at any concentrations of Pep-1. The addition of Pep-1 to negatively charged GUVs in water did not improve the binding efficiency of transferrin. No edge-specific binding to the supported bilayer was detected either (Figure 7).

Neither did $F(ab)_2$ or ovalbumin show any association with the membranes in presence (20:1−50:1 peptide/protein molar ratio, 1.7×10^{-8} M final concentration of the protein) or absence of Pep-1 for both neutral and negatively charged membranes at low and physiological ionic strengths.

Simultaneous monitoring of the fluorescence from the labeled peptides HL-Pep and AF-Pep and the labeled proteins

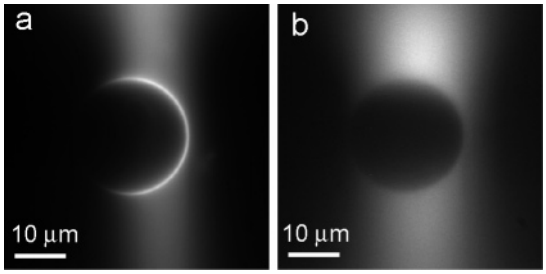

FIGURE 8: Simultaneous monitoring of HL-Pep at 488 nm (a) and labeled ovalbumin at 568 nm (b). Fluorescence of the equatorial cross sections of a POPC/POPS (2:1) GUV in 0.2 M glucose, 10 mM Hepes buffer in the presence of a mixture of fluorescently labeled HL-Pep and ovalbumin (20:1).

clearly demonstrated the absence of protein/peptide associations: for example, although AF-Pep was efficiently bound to a negative membrane as proved by its fluorescence detected in the 488 nm channel (Figure 8a), ovalbumin remains free floating in the solution as seen from the fluorescence in the 568 nm channel (Figure 8b). A similar effect was detected with neutral membranes: there was no association of the ovalbumin while HL-Pep was bound to the membrane.

In summary, Pep-1 does not assist in the binding of any of the studied proteins to model membranes over the whole stated range of experimental conditions.

DISCUSSION

Polylysine-induced fusion and aggregation of negatively charged vesicles (*23*, *24*) depend on the charge on the vesicle and the polycation and are often accompanied by leakage of the vesicle content. Pep-1 has six cationic residues, five lysines and one arginine, in sequence. Previously, vesicle aggregation and fusion induced by the peptide were detected to be significant only if the peptide concentration exceeded 6.88 μM (*6*). In our experiments the formation of aggregates was also detected, and it was easily visualized even at less than 1 μM concentration of Pep-1. We observed a Pep-1 enhanced fusion of vesicles to form a uniform bilayer. Thus, the peptide not only causes the appearance of larger vesicles due to fusion or aggregation of smaller ones but also results in sedimentation of vesicles and formation of a flat bilayer on glass. Free lateral diffusion of lipids in the bilayer, confirmed by FRAP experiments, demonstrates that the LUV membranes form an extended flat bilayer. These results are hard to reconcile with previous reports that Pep-1 does not cause leakage of LUVs (*6*, *7*). However, the sedimentation and fusion of the LUV to a flat bilayer are likely to be dependent on properties of the material used to form the sample chamber. The clean glass used in our experiments bears negatively charged groups that attracts the cationic part of the peptide and leads to adsorption of a significant amount of the peptide to the glass surface and sedimentation of anionic vesicles. The permanent attachment of peptides to glass and/or vesicles fused into a flat bilayer may also influence steady-state fluorescence measurements in bulk, such as those based on intrinsic fluorescence of tryptophans (*6*, *8*, *10*).

Bilayer destabilization and fusion of low-curvature membranes of giant vesicles induced by Pep-1 were clearly demonstrated in our observations (Figure 2). Even a low concentration of the peptide (<1 μM) caused changes in shape, fusion, and formation of internal vesicles. Headgroup charge redistribution and/or lateral tension (*25*) in the membrane may be responsible for fusion between two vesicles and for changes in the local membrane curvature leading to the formation of invaginations that subsequently detach into the interior of the GUV. Although the cell membrane is more stable because of the support of filaments and organization of lipids in the membrane by cholesterol, the formation of invaginations triggering endocytic uptake is one proposed mechanism of peptide/protein internalization (*7*).

As a primary step, entry of the CPP into the cell cytoplasm requires its association to the surface of the lipids. There are now many experiments on model membranes that address the nature of this association. The aromatic tryptophan residues of the Pep-1 sequence are energetically favorable for insertion in the neutral lipid membrane (*26*). It has been shown that the hydrophobic end of unstructured Pep-1 adopts an α-helical conformation in the presence of micelles or lipid vesicles (*8*), while the C-terminal region remains unstructured. These conclusions were based on fluorescence quenching of the Pep-1 tryptophans in the presence of phospholipid vesicles. A model was proposed in which the helical axis of the peptide is perpendicular to the membrane plane and all tryptophans are completely inserted into the lipid core. In contrast, spin-label data indicate Pep-1 lying flat on the membrane surface (*7*). The extent of partition of the Pep-1 tryptophan residues into the membrane was also examined by means of fluorescence quenching with doxyl-derivatized stearic acid (*10*). The results showed that the tryptophans are located near the water/lipid interface. A study of the tryptophan emission quenching and its blue shift in the presence of lipid vesicles (*8*, *10*) concluded that Pep-1 is anchored via tryptophans to a neutral bilayer. The surface pressure of POPC water/air monolayers is altered by the addition of the peptide, suggesting that Pep-1 is inserted into the monolayer (*8*). DPC/SDS micelles (*7*) associated with Pep-1 also show anchored tryptophan residues. Strikingly, the high affinity of Pep-1 to neutral vesicles was strongly dependent on the presence of phosphine reductant (*10*).

We have found different binding affinities for HL-Pep and AF-Pep to the neutral (POPC) membrane. While there is no association of the AF-Pep to the neutral bilayer, the HL-Pep does bind to the neutral bilayer at all ionic strengths. The difference in the interaction of these two peptides with neutral phospholipids in the bilayer suggests that solely hydrophobic interactions of aromatic residues are not responsible for binding. The unmodified tryptophan-rich hydrophobic part of the AF-Pep does not differ from the same domain of the Pep-1 so binding of those two peptides should be similar if it is assumed that the fluorescent label of the AF-Pep does not alter properties of the remote residues responsible for hydrophobic interaction. In contrast to AF-Pep, the HL-Pep does have modifications at the hydrophobic end while its C-terminal end, including the cysteamine residue, is unmodified. If it is assumed that the six methylene groups and the Hilyte fluorescent dye do not themselves interact with the bilayer, it can be concluded that the cysteamine moiety is essential for the peptide association. Similar observations were discussed in ref *11*, where the insertion of a carboxyfluorescein group at the C-terminus

of the peptide significantly reduced partitioning of the peptide into an LUV membrane.

The binding of HL-Pep was much more efficient at the edges of the supported membrane (Figure 5a). Pep-1 interaction with the hydrophobic core may be facilitated by the high curvature at the membrane edges or at defects where the close packing of the lipids is disturbed and the lipid core is more easily accessed from the exterior medium. A similar explanation was advanced for the enhanced interaction of proteins with highly curved SUV membranes (*27*).

The efficiency of binding to the unperturbed bilayer, where the tightly packed hydrophilic heads of the lipids can prevent access to the core, is much lower. We also observed formation and migration of large clusters of HL-Pep along the POPC GUV surface. A number of diffusion coefficients were observed, implying the presence of clusters having different sizes. In the example shown in Figure 4, the diffusion coefficients are 0.3 and 1 $\mu m^2/s$. The peptides appear to bind efficiently to defects which have accessible hydrocarbons. This is the case for both supported bilayers or GUVs. Recent data on lateral diffusion (*28*) in membranes have predicted an inverse relation between the diffusion coefficient and the radius of the diffusing particle. Given that the diffusion coefficient of a single lipid in a liquid-phase bilayer is about 3−5 $\mu m^2/s$ (*20*), the radius of the cluster is estimated to span 30−100 lipid molecules.

Self-association of the peptide trough its disulfide bridges has also been invoked as a factor in the binding affinity (*10*). If this were the case, we could expect TCEP reductant to influence binding. However, TCEP had no effect on the interaction of HL-Pep with the GUV membrane in any of the environments that were examined in the present work.

The importance of nonspecific electrostatics as a driving force for peripheral membrane association has been well established (see, for instance, ref *29*). The Coulomb attraction is long-range compared with hydrophobic interactions. It may serve as the initial step in peptide association (*7*, *30*), where the electrostatic attraction is followed by a hydrophobic interaction or anchoring. We clearly observed electrostatically enhanced binding of both HL-Pep and AF-Pep peptides. The addition of acidic lipids results in the peptides being strongly attached to the membrane in low ionic strength environments. The electrostatic interaction is so efficient that almost all of the peptides remain bound to the membrane surface permanently so that the effect saturates (Figure 3c). The FRAP experiments (Figure 6) confirm that after photobleaching the recovery appears exclusively in the bilayers having regions that were not exposed to the excitation beam: the bilayer shown in the center of Figure 6a was totally exposed and shows no recovery. The experiment demonstrates that the peptide associates with the charged bilayer for longer than the duration of the experiment. The population of the prebleached areas of the bilayer is maintained by the diffusion of fluorescent peptides permanently attached to the lipids of the membrane. However, the binding capacity is not saturated, because after addition of a new aliquot of the HL-Pep all membranes again become associated with the peptide (Figure 6d). Our data indicate that close to 100% partitioning of Pep-1 to charged membranes occurs. This conclusion is in agreement with previous reports (*10*).

The exponentially decaying electric field originating from the charged bilayer is shielded by counterions if they are present in the solution. The Debye screening length (*31*) decreases by about three times, from 3 nm to approximately 1 nm, when the monovalent salt concentration increases from 10 to 100 mM. We observed a strong dependence on NaCl concentration of the binding efficiency of AF-Pep and HL-Pep to GUVs (Figure 3d). The electrostatic attraction of the peptides to the anionic membranes was completely supressed at a high enough concentration of ions, demonstrating that the charged residues of the peptide are kept at distances from charged membranes comparable with the Debye length. The importance of the Coulomb attraction was also well pronounced in ref *10*, where it was shown that the introduction of anionic lipids into the membrane changes the extent of partition by an order of magnitude. However, unlike our data, the partitioning of Pep-1 to anionic LUVs decreases by less than 30% in response to changes of salt concentration from 150 to 10 mM. We verified that the effect of the ionic strength also occurs with supported bilayers, in which case the same bilayer could be exposed to different environments. The error in the GUV experiments is large because each measurement required a different vesicle. The HL-Pep readily associates with the anionic bilayer at zero salt concentration (Figure 5c), but almost no binding was detected in high ionic strength solutions (Figure 5b). Therefore, the trend is similar to the results with the GUV membrane model.

Pep-1 assisted deliveries of various proteins in the cytoplasm of different cell lines were described previously in terms of a noncovalent binding of protein and peptide(s) (*2*, *4*, *32*, *33*). These investigations were based on a statistical analysis of the translocation capacity of labeled proteins in live cells at various peptide/protein ratios. It has been reported that cargoes having a range of surface charge and hydrophobicity were successfully transferred into living cells (*2*, *4*, *5*) with a labeling ratio from 6−8:1 for a short peptide (*2*) to 6000:1 for quantum dots (*5*). The formation of complexes was verified in vitro by size exclusion chromatography (*2*) and bulk steady-state spectroscopy by means of intrinsic tryptophan quenching (*8*). The formation of stable complexes requires strong interaction forces. Originally, it has been suggested that noncovalent, hydrophobic interactions are responsible for the formation of stable peptide/cargo complexes regardless of the specific peptidyl sequence (*34*). Later it has been proposed that Pep-1 can establish a variety of electrostatic and/or hydrophobic and/or hydrophilic interactions with the cargo (*4*).

In the present work the ability of Pep-1 to induce adsorption of several proteins such as human transferrin, ovalbumin, and $F(ab)_2$ fragment of goat anti-mouse IgG was tested. All of these proteins have multiple hydrophobic residues on their surfaces. Transferrin is almost electrically neutral, while ovalbumin has a negative charge [pI = 4.7 (*22*)] and may form complexes with positively charged peptides through both hydrophobic and electrostatic interactions. We did not detect assisted binding for any of these proteins to either anionic or neutral membranes at any of the tested ionic strengths, even those where the peptide is strongly associated with the membrane (Figure 7).

While the sensitivity and time resolution are adequate to detect single fluorophores (*16*), none were detected. We did not detect any peptide-induced adsorption, but this does not necessarily imply that peptide/protein complexes are absent in the solution. Freely diffusing species are not detected

because of fast diffusion. For instance, efficient complexation of the cationic tail of Pep-1 with anionic ovalbumin would be expected, but this association may compensate the charges required for binding to the membrane, thus preventing the association and immobilization of preformed complexes to the membrane surface.

Translocation of fluorescently labeled peptides and protein/peptide complexes through the GUV membrane did not occur in our experiments. Although a transmembrane potential is supposed to be an efficient driving force for translocation (*6*), it is unlikely that the gradient influences the association of the peptide to the membrane upon which the overall efficiency of translocation must depend.

CONCLUSIONS

In the present study, we concentrated on several aspects of the interaction of a cell-penetrating peptide Pep-1 with model membranes at the single-molecule level. In contrast to previously published data in bulk media, we performed single-molecule imaging experiments, which allow us to eliminate concentration-dependent effects and possible phenomena caused by the interaction with the glass walls of the measuring cell.

The effectiveness of Pep-1 in inducing changes in lipid membranes, undergoing association with neutral and charged bilayers, and assisting in the binding of proteins to the membrane was visualized by direct fluorescent imaging methods. Membranes of large and giant unilamellar vesicles and flat supported bilayers were used as models. Native Pep-1 and two designed fluorescent analogues of Pep-1 with labeling chosen to minimize possible alteration of the peptide functionality were used in the experiments.

We discussed the various mechanisms of hydrophobic and/or electrostatic attraction of the peptide with charged and neutral membranes. Direct comparison of the Pep-1 peptide analogues labeled at C- (HL-Pep) and N- (AF-Pep) termini reveals the significant difference in the adsorption. Summarizing our observations on the interaction of the peptide with neutral membranes, we can conclude that the tryptophan interaction (*7*, *10*, *32*) is certainly not the only mechanism responsible for peptide association. The primary anchoring of the cysteamine moiety is identified as a necessary step in the process of association. The electrostatic attractive forces are shown to be important in the binding of the peptide, but they are almost completely diminished at physiologically important ionic strengths and perhaps do not play an important role in the association of the peptide with the surface of living cells.

It has been shown that Pep-1 is a strong perturber of lipid membranes and causes changes in the membrane of cell-sized giant vesicles, induces sedimentation of LUVs to a glass surface, and leads to fusion of vesicles into a flat lipid bilayer. Furthermore, it was also demonstrated that defects in the lipid organization of the membrane are very efficient in enabling association with the peptide. We did not detect any translocation of the peptides through the membrane. No Pep-1 induced binding to LUVs or GUVs was detected for the proteins human transferrin, ovalbumin, and $F(ab)_2$.

The translocation ability of peptide/cargo complexes is widely discussed in the literature, and almost all models require many copies of Pep-1 to be associated with the cargo. Translocation of a single CPP may not require multiple copies. Whether a transient pore, invaginations promoted by the peptide, or other membrane alterations are responsible for translocation is not yet clear.

We conjecture from single-molecule measurements that Pep-1 (no cargo) interacts in a cooperative manner with the membrane that then would influence translocation of cargo. It is likely that Pep-1 causes the formation of invaginations that trigger the endocytic uptake as proposed in ref *7*.

ACKNOWLEDGMENT

We are indebted to Prof. Fred Schroeder and Prof. Kevin Burgess for valuable discussion and for introducing us to the Chariot peptide.

REFERENCES

1. Magzoub, M., and Graslund, A. (2004) Cell-penetrating peptides: small from inception to application, *Q. Rev. Biophys. 34*, 147−195.
2. Morris, M. C., Julien, D., Jean, M., Frederic, H., and Divita, G. (2001) A peptide cerier for the delivery of biologically active proteins into mammalian cells, *Nat. Biotechnol. 19*.
3. Chariot(tm), Active Motive of North America (http://www.activemotif.com).
4. Henriques, S. T., Costa, J., and Castanho, M. A. R. B. (2005) Translocation of β-galactosidase mediated by the cell-penetrating peptide Pep-1 into lipid vesicles and human HeLa cells is driven by membrane electrostatic potential, *Biochemistry 44*, 10189−10198.
5. Mattheakis, L. C., Dias, J. M., Choi, Y.-J., Gong, J., Bruchez, M. P., Liu, J., and Wang, E. (2004) Optical coding of mammalian cells using semiconductor quantum dots, *Anal. Biochem. 327*, 200−208.
6. Henriques, S. T., and Castanho, M. A. R. B. (2004) Consequences of nonlytic membrane perturbation to the translocation of the cell penetrating peptide Pep-1 in lipidic vesicles, *Biochemistry 43*, 9716−9724.
7. Weller, K., Lauber, S., Lerch, M., Renaud, A., Merkle, H. P., and Zerbe, O. (2005) Biophysical and biological studies of end-group-modified derivatives of Pep-1, *Biochemistry 44*, 15799−15811.
8. Deshayes, S., Heitz, A., Morris, M. C., Charnet, P., Divita, G., and Heitz, F. (2004) Insight into the mechanism of internalization of the cell-penetrating carrier peptide Pep-1 through conformational analysis, *Biochemistry 43*, 1449−1457.
9. Richard, J. P., Melikov, K., Vives, E., Ramos, C., Verbeure, B., Gait, M. J., Chernomordik, L. V., and Lebleu, B. (2003) Cell-penetrating peptides. A reevaluation of the mechanism of cellular uptake, *J. Biol. Chem. 279*, 585−590.
10. Henriques, S. T., and Castanho, M. A. R. B. (2005) Environmental factors that enhance the action of the cell penetrating peptide Pep-1. A spectroscopic study using lipidic vesicles, *Biochim. Biophys. Acta 1669*, 75−86.
11. Henriques, S. T., Costab, J. L., and Castanho, M. A. R. B. (2005) Re-evaluating the role of strongly charged sequences in amphipathic cell-penetrating peptides. A fluorescence study using Pep-1, *FEBS Lett. 579*, 4498−4502.
12. Johnson, J. M., Ha, T., Chu, S., and Boxer, S. G. (2002) Early steps of supported bilayer formation probed by single vesicle fluorescence assays, *Biophys. J. 83*, 3371−3379.
13. Angelova, M. I., and Dimitrov (1988) A mechanism of liposome electroformation, *Progr. Colloid Polym. Sci. 76*, 59−67.
14. Mei, E., Sharonov, A., Ferris, J. H., and Hochstrasser, R. M. (2005) Direct visualization of nanopatterns by single-molecule imaging, *Appl. Phys. Lett. 86*, 043102.
15. Mei, E., Sharonov, A., Gao, F., Ferris, J. H., and Hochstrasser, R. M. (2004) Anomalously slow diffusion of single molecules near a patterned surface, *J. Phys. Chem. A 108*, 7339−7346.
16. Sharonov, A., and Hochstrasser, R. M. (2006) Wide-field subdiffraction imaging by accumulated binding of diffusing probes, *Proc. Natl. Acad. Sci. U.S.A. 103*, 18911−18916.
17. Axelrod, D. (1989) Total internal reflection fluorescence microscopy, *Methods Cell Biol. 30*, 245−270.

18. Tokunaga, M., Kitamura, K., Saito, K., Iwane, A. H., and Yanagida, T. (1997) Single molecule imaging of fluorophores and enzymatic reactions achieved by objective-type total internal reflection fluorescence microscopy, *Biochem. Biophys. Res. Commun. 235*, 47−53.
19. Axelrod, D., Koppel, D. E., Schlessinger, J., Elson, E., and Webb, W. W. (1976) Mobility measurement by analysis of fluorescence photobleaching recovery kinetics, *Biophys. J. 16*, 1055−1069.
20. Vaz, W. L. C., Stümpel, J., Hallmann, D., Gambacorta, A., and Rosa, M. D. (1987) Bounding fluid viscosity and translational diffusion in a fluid lipid bilayer, *Eur. Biophys. J. 15*, 111−115.
21. Aveyard, R., and Haydon, D. A. (1973) *An Introduction to the Principles of Surface Chemistry*, Cambridge University Press, Cambridge, U.K.
22. Turkova, J. (1999) Bioaffinity chromatography, in *Analytical and Preparative Separation Methods of Biomacromolecules* (Aboul-Enein, H. Y., Ed.) Marcel Dekker, New York.
23. Gad, A. E., Silver, B. L., and Eytan, G. D. (1982) Polycation-induced fusion of negatively-charged vesicles, *Biochim. Biophys. Acta 690*, 124−132.
24. Walter, A., Steer, C. J., and Blumenthal, R. (1986) Polylysine induces pH-dependent fusion of acidic phospholipid vesicles: a model for polycation-induced fusion, *Biochim. Biophys. Acta 861*, 319−330.
25. Tanaka, T., and Yamazaki, M. (2004) Membrane fusion of giant unilamellar vesicles of neutral phospholipid membranes induced by La^{3+}, *Langmuir 20*, 5160−5164.
26. Wimley, W. C., and White, S. H. (1996) Experimentally determined hydrophobicity scale for proteins at membrane interfaces, *Nat. Struct. Biol. 3*, 842−848.
27. Chao, H., Martin, G. G., Russell, W. K., Waghela, S. D., Russell, D. H., Schroeder, F., and Kier, A. B. (2002) Membrane charge and curvature determine interaction with acyl-CoA binding protein (ACBP) and fatty acyl-CoA targeting, *Biochemistry 41*, 10540−10553.
28. Gambin, Y., Lopez-Esparza, R., Reffay, M., Sierecki, E., Gov, N. S., Genest, M., Hodges, R. S., and Urbach, W. (2006) Lateral mobility of proteins in liquid membranes revisited, *Proc. Natl. Acad. Sci. U.S.A. 103*, 2098−2102.
29. Mulgrew-Nesbitt, A., Diraviyam, K., Wang, J., Singh, S., Murray, P., Li, Z., Rogers, L., Mirkovic, N., and Murray, D. (2006) The role of electrostatics in protein−membrane interactions, *Biochim. Biophys. Acta 1761*, 812−826.
30. Dom, G., Shaw-Jackson, C., Matis, C., Boufioux, O., Picard, J. J., Prochiantz, A., Mingeot-Leclercq, M.-P., Brasseur, R., and Rezsohazy, R. (2003) Cellular uptake of antennapedia penetratin peptides is a two-step process in which phase transfer precedes a tryptophan-dependent translocation, *Nucleic Acids Res. 31*, 556−561.
31. Graf, K., Kappl, M., Hans-Jürgen, and Butt, B. (2003) *Physics and Chemistry of Interfaces*, Wiley-VCH, New York.
32. Deshayes, S., Morris, M. C., Divita, G., and Heitz, F. (2006) Interactions of amphipathic CPPs with model membranes, *Biochim. Biophys. Acta 1758*, 328−335.
33. Aoshiba, K., Yokohori, N., and Nagai, A. (2003) Alveolar wall apoptosis causes lung destruction and emphysematous changes, *Am. J. Respir. Cell Mol. Biol. 28*, 555−562.
34. Gros, E., Deshayes, S., Morris, M. C., Aldrian-Herrada, G., Depollier, J., Heitz, F., and Divita, G. (2006) A noncovalent peptide-based strategy for protein and peptide nucleic acid transduction, *Biochim. Biophys. Acta 1758*, 384−393.

BI700505H